J Mater Sci (2015) 50:4430–4439
DOI 10.1007/s10853-015-9011-3

Effects of incoherent nanoinclusions on stress-driven migration of low-angle grain boundaries in nanocomposites

I. A. Ovid'ko[1,2,3] · A. G. Sheinerman[1,2,3]

Received: 20 February 2015 / Accepted: 6 April 2015 / Published online: 10 April 2015

Abstract Stress-driven migration of grain boundaries (GBs) is theoretically described as a plastic deformation mode in metal matrix nanocomposites containing incoherent reinforcing (ceramic or metallic) nanoinclusions. We considered the exemplary case of low-angle tilt boundaries migrating in nanocrystalline or ultrafine-grained metallic matrixes and analytically calculated the effects of reinforcing nanoinclusions on the GB migration process. In doing so, migrating low-angle tilt boundaries are represented as walls of edge lattice dislocations that cooperatively glide in a metal matrix but cannot penetrate wire nanoinclusions. It is theoretically revealed that the nanoinclusions typically hamper the stress-driven GB migration. At the same time, in the situation with small (ultrafine) nanoinclusions, they cause an anomalous effect enhancing (or, in other terms, decreasing the critical stress for unlimited migration) the stress-driven GB migration in metal–metal and metal–ceramic nanocomposites. The results of our theoretical examination are consistent with the corresponding experimental data reported in the literature.

✉ A. G. Sheinerman
asheinerman@gmail.com

I. A. Ovid'ko
ovidko@nano.ipme.ru

[1] Research Laboratory for Mechanics of New Nanomaterials, St. Petersburg State Polytechnical University, St. Petersburg 195251, Russia

[2] Department of Mathematics and Mechanics, St. Petersburg State University, St. Petersburg 198504, Russia

[3] Institute of Problems of Mechanical Engineering, Russian Academy of Sciences, Bolshoj 61, Vasilievskii Ostrov, St. Petersburg 199178, Russia

Introduction

The nanoscale and interface effects crucially influence plastic deformation mechanisms/modes operating in nanocrystalline (NC) and ultrafine-grained (UFG) bulk materials, ultrathin films, and nanowires showing excellent mechanical properties (see, e.g., [1–11]). For instance, in NC and UFG metallic materials, conventional lattice slip is hampered by large amounts of grain boundaries (GBs), in which case plastic flow often occurs through alternative deformation modes mediated by GBs (see, e.g., [4]). In particular, the stress-driven athermal migration of GBs is recognized as one of the alternative deformation modes effectively operating in NC and UFG metals in wide range of their structural parameters [4, 12–34]. The stress-driven GB migration leads to grain growth that destroys the NC/UFG structure of metals and thus results in degradation of their properties attributed to such a structure.

In general, conventional thermally activated grain growth is viewed as the key negative factor that can come into play in NC/UFG metals during their fabrication and thus destroy their NC/UFG structure [4]. In order to inhibit the thermally activated grain growth, several approaches are utilized which are also typical for microcrystalline and coarse-grained polycrystals [35, 36]. Among the most effective approaches is the use of nanoinclusions (like nanoscale precipitates of the second metallic phase in metallic alloys and second-phase ceramic nanoparticles in metal matrix nanocomposites) as obstacles for GB migration (see, e.g., [4, 37, 38]). In addition to their role as inhibitors of thermally activated grain growth, nanoinclusions serve as reinforcing structural elements that hinder lattice dislocation slip (see, e.g., [8, 39, 40]) and affect crack growth [41–43].

At the same time, the research efforts focused on the effects exhibited by nanoinclusions on the stress-driven GB

migration in NC and UFG metallic materials are limited. In particular, very recently, the effects of Al_2O_3 ceramic nanoinclusions on both stress-driven GB migration and grain growth processes in nanostructured Al matrix and Al alloy matrix nanocomposites have been experimentally examined by Lin with co-workers [44, 45]. In their works, nanocrystalline Al having an initial grain size of 79 nm and containing 13 vol% of Al_2O_3 nanoparticles with an average size of 27 nm, has been extruded at a temperature of 400 °C with the strain rate of 0.6 s^{-1} until an area reduction of 9–10. Hot extrusion of nanocrystalline Al containing Al_2O_3 nanoparticles resulted in significant grain growth (up to grain size of 177 nm). In the situation without extrusion, essential grain growth has not occurred even after annealing at a higher temperature of 600 °C. In another experiment, Dám et al. [46] observed stress-driven migration of low-angle GBs in the ultrafine-grained (with a grain size of 200–300 nm) Al-3 Mg-0.2Sc (wt%) alloy, containing coherent nanoscale (3–5 nm in diameter) Al_3Sc precipitates, during tensile deformation at 300 °C. At the same time, in the experiment [46], the migration of high-angle GBs has not been observed.

Also, a model of stress-driven grain growth hampered by ceramic nanoinclusions in nanostructured Al matrix nanocomposite was suggested [45, 47]. Also, stress-driven migration of low-angle grain boundaries in the presence of rigid impenetrable precipitates has been simulated using 3D discrete dislocation dynamics [48]. However, models [45, 47, 48] are too simple because they do not involve in examining the role of GB junctions in stress-driven GB migration. At the same time, the effects of GB junctions on thermally activated and especially stress-driven GB migration processes are critical in NC and UFG materials specified by extremely large amounts of triple junctions of GBs (see, e.g., [14, 21, 23, 28, 49–51]). The main aim of this paper is to theoretically describe the stress-driven GB migration as a plastic deformation mode in metal matrix nanocomposites containing incoherent reinforcing (ceramic or metallic) nanoinclusions, with the role of GB junctions taken into consideration. The focuses of our examination will be placed on the effects of such nanoinclusions on both the critical stresses for the GB migration processes and profiles of migrating GBs in these metal matrix nanocomposites. In particular, we will reveal the dependences of the critical stress on nanoinclusion sizes.

Stress-driven migration of low-angle grain boundaries in metal–ceramic and metal–metal nanocomposites: geometric aspects

Let us consider a nanocomposite solid consisting of an NC/UFG metal matrix and incoherent reinforcing (metallic or ceramic) nanoinclusions (Fig. 1). We examine the situation where a mechanical load is applied to the nanocomposite and drives GB migration in the metal matrix of the nanocomposite. For definiteness and simplicity, our consideration will be focused on stress-driven migration of low-angle tilt boundaries conventionally represented/modeled as walls of edge lattice dislocations. Due to the high Peierls barrier for dislocation slip in the ceramic nanoinclusions and the difference in the types of the crystal lattices between the matrix and the metallic nanoinclusions, migrating GBs cannot penetrate the nanoinclusions. Instead, GBs are bent around the incoherent nanoinclusions. In doing so, the migrating GBs can either stop at nanoinclusions or move further, depending on the applied load as well as both the geometry and the size of the GBs and nanoinclusions.

In order to calculate the critical parameters at which a migrating GB can bypass a nanoinclusion, we consider a symmetric low-angle tilt boundary terminated at triple junctions, A and B, of GBs in a composite solid in its initial state before the migration (Fig. 2a). Although, in general, migrating low-angle GBs can be of an arbitrary (tilt, twist, or mixed) type, we focus our consideration on the most widespread tilt boundaries. Each such boundary consists of edge dislocations and can easily migrate, as compared to twist and mixed GBs. In the initial state, in the absence of a mechanical load, the low-angle boundary AB is represented as a straight wall of periodically arranged edge dislocations having the same Burgers vector $\boldsymbol{b}$. The low-

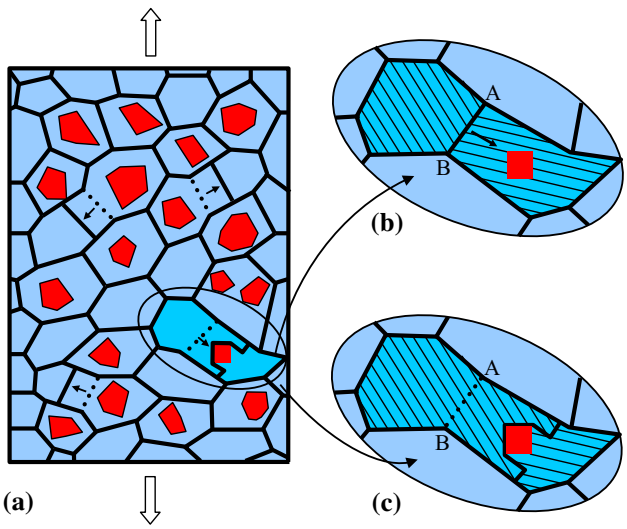

Fig. 1 (Color figure online) Stress-driven migration of a grain boundary in a nanocomposite solid containing hard (ceramic or metallic) nanoinclusions inside grains of a metallic matrix. **a** A nanocomposite specimen is under a mechanical load (a two-dimensional general view.). **b** The *magnified region* [bounded by an *ellipse* in (**a**)] highlights the initial state of the nanocomposite, before the grain boundary migration. **c** The *magnified region* [bounded by an *ellipse* in (**a**)] highlights the final state of the nanocomposite, after the stress-driven grain boundary migration

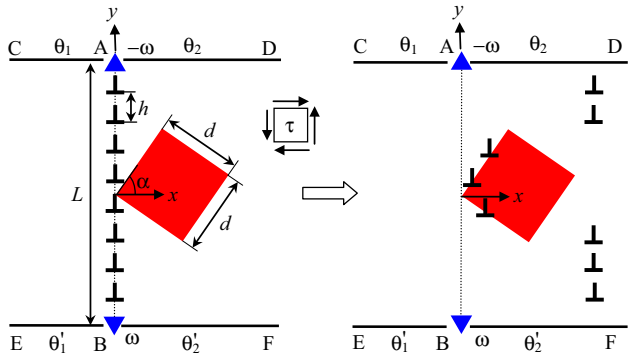

Fig. 2 (Color online) Migration of a low-angle tilt boundary near an incoherent nanoinclusion impenetrable for dislocations

angle boundary is characterized by the tilt misorientation angle θ being in the Frank relationship $[\sin(\theta/2) = b/(2h)]$ [52] with the parameters (period h and Burgers vector magnitude b) of the dislocation arrangement in the boundary.

In the initial state before the migration process, other GBs (AC, AD, BE, and BF) adjacent to the GB AB are assumed to be symmetric tilt boundaries that form the geometrically compensated triple junctions A and B with the boundary AB (Fig. 2a). The triple junctions A and B are geometrically compensated in the sense that there are no angle gaps at these junctions. In other words, the sum of tilt misorientation angles of all GBs joining at each of these junctions is equal to zero, where summation of the angles is performed clockwise along a circuit surrounding a triple junction [53, 54]: $\theta + \theta_{AC} + \theta_{AD} = 0$ and $-\theta + \theta_{BF} + \theta_{BE} = 0$. Here θ_{AC}, θ_{AD}, θ_{BF}, and θ_{BE} are the tilt misorientation parameters of the GBs AC, AD, BF, and BE, respectively (Fig. 2a). In the situation under examination, we will consider the dislocation structures of the GBs AC, AD, BE, and BF to be unchanged during the stress-driven migration of the GB AB (Fig. 2). In this situation, the GBs AC, AD, BE, and BF cooperatively serve as constant stress sources located at triple junctions and balanced in the initial state (Fig. 2a). More precisely, following the approach [14, 21, 23], the GBs AC and AD are modeled as a wedge disclination located at the triple junction A and characterized by the disclination strength $-\omega = -\theta$ (Fig. 2a). The GBs BF and BE are modeled as a wedge disclination located at the triple junction B and characterized by the disclination strength $\omega = \theta$ (Fig. 2a).

We now consider migration of the GB AB under the applied shear stress τ in the nanocomposite. When the shear stress τ acts in slip planes of the lattice edge dislocations belonging to the GB AB, these dislocations cooperatively glide from their initial positions (Fig. 2a) to the new positions (Fig. 2b). These stress-driven cooperative displacements of the dislocations result in the migration of the GB AB (Fig. 2b). Within our two-dimensional model, we assume that the migrating GB is retarded by a wire nanoinclusion having both a square cross section and the long axis normal to the plane of Fig. 2 (and parallel with dislocations lines that form the migrating GB). Within the model, the sides of the square that forms the nanoinclusion cross section have the length d, and one of the square sides makes the angle α with the normal to the GB plane (Fig. 2). Also, since the inclusion is assumed to be incoherent, it is not strained to adjust the matrix and does not create any elastic stresses. Besides, since the inclusion is incoherent, it is assumed to be impenetrable for dislocations that form the dislocation wall. The effect of coherent inclusions (that both create elastic stresses and are penetrable for dislocations) on GB migration is considered elsewhere [55]. As the main role of the inclusion is in retarding dislocations, we believe that its exact shape is not important. Therefore, although here, for definiteness, we have modeled the inclusion as a square, we believe that its effect on GB migration will be qualitatively the same for other (e.g., elliptic) shapes of the inclusion. In general, the inclusion–matrix interface can exert elastic forces on dislocations if the matrix and inclusions have vastly different elastic moduli (due to the dislocation attraction to the softer phase). However, in our manuscript, we focus our consideration on the situation where the elastic moduli of the matrix and inclusions are sufficiently close to each other, and their difference can be neglected.

Stress-driven migration of low-angle grain boundaries in metal–ceramic and metal–metal nanocomposites: stress characteristics and profile of a migrating grain boundary

Let us examine the process of the stress-driven migration of the low-angle GB AB meeting an incoherent nanoinclusion in a metal matrix nanocomposite. For definiteness, we focus our examination on the case of low homological temperatures. In this case, one can neglect the effects associated with the thermally assisted GB migration, in particular, diffusional accommodation of the stresses produced by triple junction disclinations. Besides, in this case, due to the low diffusion rate, the inclusion is immobile and cannot move together with the migrating GB. In our analysis, we will exploit the methods of the two-dimensional discrete dislocation dynamics approach employed previously for description of the formation, decay or evolution of GBs (see, e.g., [56–59]). The two-dimensional dislocation dynamics approach is a partial case of the 3D discrete dislocation dynamics method (see, e.g., [60–63]). Although 3D simulations are most effective for a detailed comprehensive analysis of migration of low-angle GBs in solids containing inclusions/precipitates, the 2D approach

definitely catches essential physics of the GB migration process and, at the same time, does not need excessively complicated analytical calculations and/or computer simulations. Within the approach in question, each dislocation at the low-angle GB AB is under the combined actions of the forces created by the shear stress, other dislocations belonging to the boundary, and the disclination dipole.

We now calculate these forces and write the corresponding equations for dislocation motion. To do so, we assume that dislocations can move along one slip plane (along the x-axis in the coordinate system shown in Fig. 2), and, therefore, only the projections of the forces on the x-axis matter. In these circumstances, the solution of the system of equations, describing one-dimensional motion of dislocations, will be expressed as dependences $x_i(t)$, where x_i is the coordinate of the ith dislocation ($i = 1, \ldots, N$), and t is time. Also, in our examination, in a first approximation, we neglect the difference in the elastic moduli between the nanoinclusions and the matrix and model the nanocomposite as an elastically isotropic, homogeneous solid characterized by the shear modulus G and Poisson's ratio ν. Also, in our two-dimensional model, we assume that if a dislocation approaches the inclusion, it stops. We, therefore, neglect the possibility for dislocations to pass the inclusion by bowing out or by double cross-slip.

With the assumption under examination, our theoretical analysis can be extended to the situation with metal matrix nanocomposites containing incoherent nanoparticles in a NC matrix (Fig. 3). In this situation, the length of moving dislocation segments is small, which prevents these segments from bypassing isolated particle-like nanoinclusions in nanograins. At the same time, if some dislocations can bypass nanoinclusion(s), the above assumption can lead to an overestimate of the effect of nanoinclusions on the critical stress for GB migration.

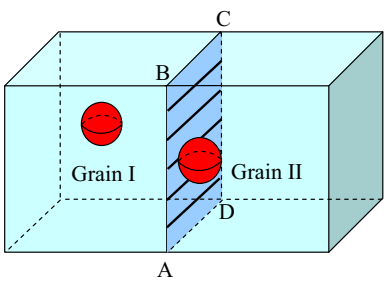

Fig. 3 (Color online) Fragment of a composite solid containing a low-angle grain boundary ABCD (with an array of dislocation segments) and spherical inclusions (whose size is comparable to the width of the grain boundary), illustrating the situation where grain boundary dislocations cannot bypass inclusions

Within the approach under discussion, the projection F_i of the total force acting on the ith dislocation belonging to the GB AB is written as follows [56]:

$$F_i = b\tau + Db^2 \sum_{\substack{k=1 \\ k\neq i}}^{N} \frac{(x_i - x_k)\left[(x_i - x_k)^2 - (y_i - y_k)^2\right]}{\left[(x_i - x_k)^2 + (y_i - y_k)^2\right]^2} - Db\omega\left(\frac{x_i(y_i + L/2)}{x_i^2 + (y_i + L/2)^2} - \frac{x_i(y_i - L/2)}{x_i^2 + (y_i - L/2)^2}\right), \quad (1)$$

where $D = G/[2\pi(1-\nu)]$, L denotes the GB length (the distance between the triple junction disclinations that form the dipole (see Fig. 2)), while x_i and $y_i = h(i - 1/2) - L/2$ are the coordinates of the ith dislocation. The first term on the right-hand side of formula (1) describes the force created by the shear stress τ, the second term describes the force of the interaction of the ith dislocation with the other dislocations of the boundary, and the third term describes the force of the interaction of the ith dislocation with the disclination dipole. In other words, the third term characterizes the role of GB junctions in the stress-driven GB migration.

The equations for the motion of dislocations composing the dislocation wall (low-angle tilt boundary) AB have the following form:

$$m\frac{d^2x_i}{dt^2} + \beta\frac{dx_i}{dt} = F_i, \quad i = 1, \ldots, N. \quad (2)$$

The first derivatives dx_i/dt in these equations take into account the dislocation motion friction (associated with the dynamic retardation of the crystalline lattice to the dislocation glide), and β is the viscosity coefficient. The dislocation mass m is given by the standard approximation [55] as $m = \rho b^2/2$, where ρ is the material density.

With Eqs. (1) and (2), we simulated the motion of the low-angle tilt boundary AB in the presence of a nanoinclusion. In the simulations, it was assumed that if a dislocation approaches the boundary of the nanoinclusion, it stops. At the same time, any i th dislocation can move back from the nanoinclusion boundary if the projection F_i of the total force acting on this dislocation becomes negative. Our analysis has demonstrated that similar to the case of GB migration in single-phase metallic solids [14], GB motion in the nanocomposite can occur in two different modes. In the first mode, all the dislocations eventually approach their equilibrium positions, and we refer to this mode as the limited GB migration. In the second mode, some dislocations stop at the nanoinclusion boundary, while others move unrestrictedly far away from it. We define this mode as the unlimited GB migration (Obviously, in reality, the unlimited migration of a GB is eventually stopped when this boundary meets a neighboring GB). Thus, in the simulations of dislocation motion, with Eqs. (1) and (2), we stop the simulations in the

two following situations. In the first situation, the displacements of all the dislocations at a given simulation step is smaller than a preset value, that is, all the dislocations have reached their equilibrium positions corresponding to the limited mode of GB migration. In the second situation, corresponding to the unlimited mode of GB migration, some dislocations are retarded by the nanoinclusion boundary, whereas other dislocations move far enough from their initial positions.

With the calculated positions of the dislocations, we revealed the profiles of the migrating GB AB in various cases. Figures 4 and 5 show these profiles in the case of a composite solid with the titanium matrix, for the following values of parameters: $G = 44$ GPa, $\nu = 0.32$, $b = 0.295$ nm and $\rho = 4506$ kg m^{-3}. Also, following [64], we take the value of β as $\beta = 5 \times 10^{-5}$ Pa $\times$ s as well as put the values of other parameters as follows: $\alpha = 45°$, $\omega = 5°$, and $N = 30$. The latter number of dislocations at the GB AB corresponds to the GB length of $L \approx 101$ nm. Note that, according to our examination (that is, according to numerical computation of the equilibrium GB profiles at various ratios of d/L), for a given value of the applied shear stress, the equilibrium profiles of the GB in the normalized coordinates $(x/d,y/d)$ do not change, when the number N of dislocations changes, but the ratio d/L is constant. This means that the profiles of the migrating GBs are not sensitive to both the GB size L and the nanoparticle size d as separate parameters, but they are influenced by the ratio d/L.

Figure 4a, b present the simulated equilibrium profiles of the migrating GB, for $d/L = 0.3$ and two different values of the applies shear stress τ. It is seen that the migrating GB is bent around the inclusion. Also, from Fig. 4, it follows that the GB migration length grows with the increasing applied stress τ. When the stress τ reaches its critical value τ_c, the limited GB migration switches to the mode of unlimited migration, in which case the middle segment of the migrating GB is stopped by the nanoinclusion and separates from the upper and lower GB segments that move in the unlimited way (Fig. 4c). In other words, the GB splits into three GB segments. The middle segment is stopped by the inclusion, while the upper and lower segments (that move above and below the inclusion, respectively) are mobile. Obviously, the size of the middle GB segment (which is bent around the nanoinclusion) is smaller than the size of the whole migrating GB in Fig. 4a, b. Since the characteristic equilibrium migration length of a GB decreases with the decreasing GB length [14], the equilibrium migration length for the middle GB segment is smaller than that for the whole GB. As a result, with time, this GB segment moves back toward the initial position of the migrating GB (Fig. 4c).

It should be noted that there is an analogy between the presence of the critical stress for unlimited GB migration and that for dislocation interactions with obstacles. Below some critical stress, the force acting on the migrating GB due to the applied stress can be balanced by both the returning force created by the disclination dipole and the capillary force of the curved boundary (which bows out between the neighboring GBs or between a GB and a precipitate), and the motion stops. Above the critical stress, even the maximum GB curvature (together with the disclination dipole) cannot balance the stress and the boundary moves unlimitedly.

Figure 5 shows (a) equilibrium and (b) nonequilibrium profiles of the migrating GB, for $d/L = 0.6$ and two different values of the applies stress τ. As it follows from Fig. 5b, if the lengths of the upper and lower segments of the migrating GB are small, their separation weakly influences the profile of the GB segment which is bent around the nanoinclusion. In this case, the length of the middle GB segment is close to that of the entire GB, and the equilibrium migration length for this GB segment is close to the equilibrium migration length of the whole GB in the absence of the nanoinclusion. As a result, a considerable reverse motion of this GB segment does not occur, in contrast to the situation illustrated in Fig. 3c.

By comparing Figs. 4b, c, and 5a, b, one can conclude that the transition from limited to unlimited GB migration occurs at some critical applied stress τ_c. Previous calculations [14] have demonstrated that in the absence of a nanoinclusion, such a transition occurs at the critical stress $\tau_c \approx 0.8D\omega$, for any materials parameters. Our analysis has demonstrated that in the examined case of a nanocomposite containing nanoinclusions, the ratio $\tau_c/(D\omega)$ also does not depend on the material parameters, but is sensitive to both the ratio d/L and the angle α. The calculated dependence of $\tau_c/(D\omega)$ on d/L, for $\alpha = 45°$, is presented by the dashed line in Fig. 6. Surprisingly, it appears that for small values of d/L, the critical stress τ_c decreases with an increase in the nanoinclusion size d (from $0.81D\omega$ at $d/L = 0$ down to the minimum value of $0.67D\omega$ at $d/L = 0.09$). At the same time, for comparatively large values of d/L, the critical stress τ_c increases with increase in the ratio d/L, as one could expect.

Moreover, Fig. 6 demonstrates that the critical stress τ_c for the unlimited GB migration in the presence of a small nanoinclusion is lower than that in the absence of nanoinclusions. In order to explain this intuitively unexpected effect of nanoinclusions on the stress-driven GB migration, we calculated the profile of a migrating GB in the case of a small nanoinclusion specified by $d/L = 0.1$ and $\alpha = 45°$ (Fig. 7). In the case under discussion, Fig. 7 demonstrates that due to the small size of the nanoinclusion, the equilibrium migration distance of the upper and lower parts of the GB can be much larger than the

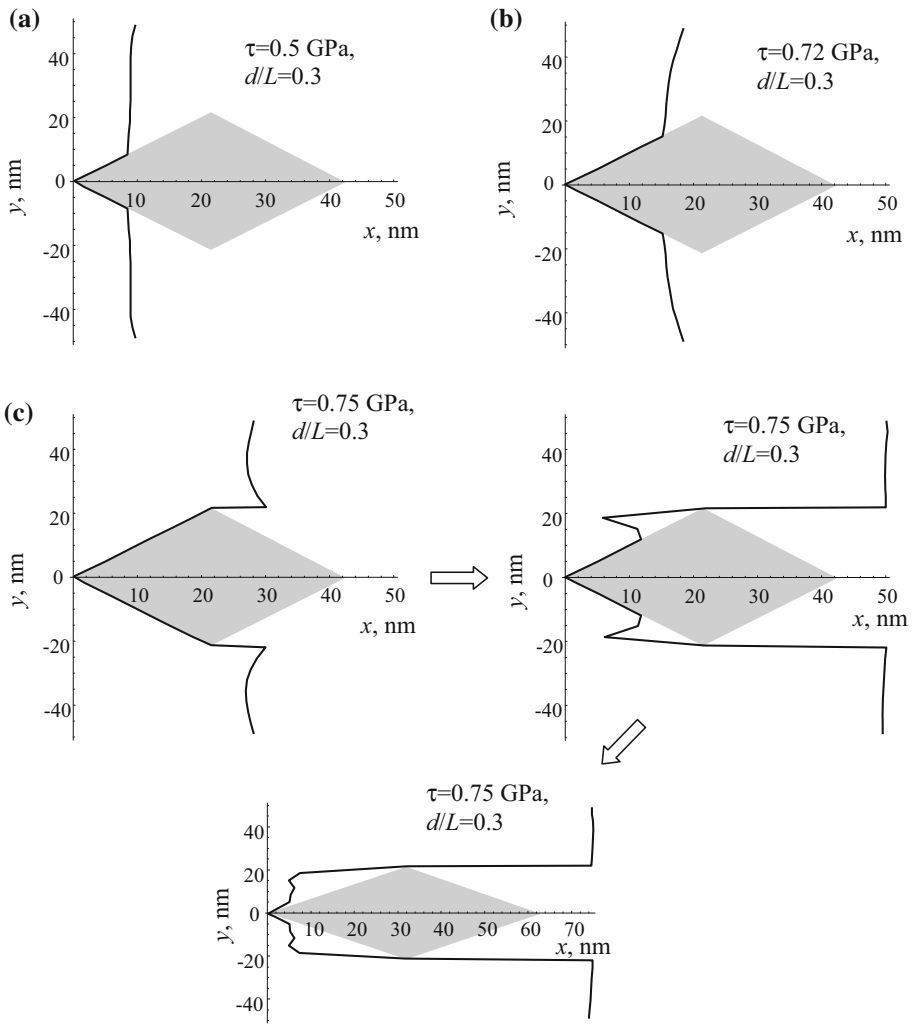

Fig. 4 Geometry of a migrating grain boundary that bends around a nanoinclusion at various values of applied stress. **a**, **b** Equilibrium profiles of a migrating grain boundary. **c** Nonequilibrium profiles of a migrating grain boundary at successive time moments

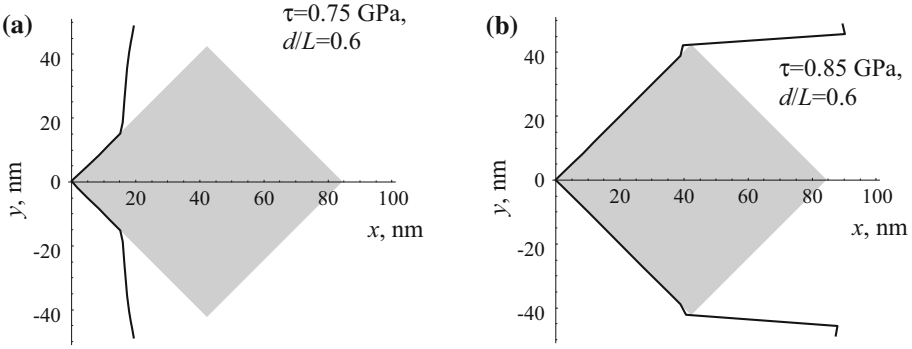

Fig. 5 Geometry of a migrating grain boundary that bends around a nanoinclusion at different values of applied stress τ. **a** Equilibrium profile of a migrating grain boundary at $\tau = 0.75$ GPa. **b** Nonequilibrium profile of a migrating grain boundary at $\tau = 0.85$ GPa

nanoinclusion size. In other words, in this situation, the lower and upper GB segments separate from the immobile middle GB segment before the GB migration switches to its unlimited mode. In this case, the distance between the middle GB segment and its upper and lower segments is large. According to the theory of dislocations [65], two edge dislocations with the same Burgers vectors directed along the x-axis (see Fig. 2b) and the coordinates (x_i, y_i) and (x_k, y_k) repel, if their lateral distance $|x_i - x_k|$ is larger than their vertical distance $|y_i - y_k|$. Thus, in the discussed case, the dislocations at the middle GB segment (stopped at the nanoinclusion boundary) repel the dislocations in the upper and lower GB segments. (It is contrasted to the case of a straight GB whose dislocations do not exert forces

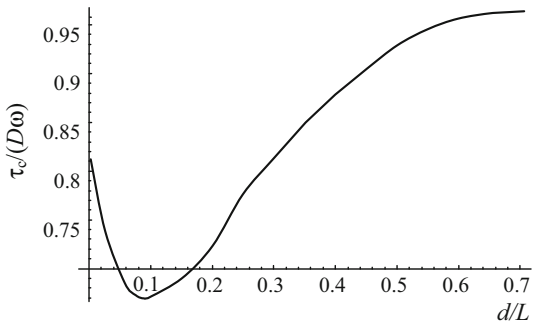

Fig. 6 Dependence of the normalized critical stress $\tau_c/(D\omega)$ for unlimited migration of a low-angle grain boundary on the ratio *d/L* of the nanoinclusion size *d* to the grain boundary length *L*

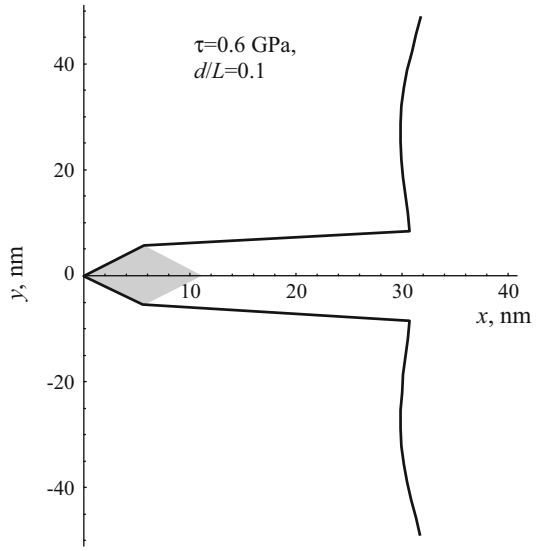

Fig. 7 Equilibrium profile of a migrating grain boundary that bends around a small nanoinclusion

along the *x*-axis on each other). As a result, the force F_i acting on these dislocations becomes larger than it would be in the case where the straight GB migrates as a whole. Therefore, the critical stress τ_c for the unlimited GB migration in the presence of a small nanoinclusion is lower than that in the situation without a nanoinclusion.

At the same time, for large enough values of the ratio d/L, the transition from the limited migration mode to the unlimited migration mode occurs at the stress level at which the upper and lower GB segments start separating from the middle one. In this situation, due to small distances between the dislocations in the middle GB segment and the dislocations in the upper and lower GB segment, the dislocations in the middle part of the GB attract the dislocations in the upper and lower GB segments (along the *x*-axis). As a corollary, the force F_i acting on the latter dislocations decreases, compared to the case where the straight GB migrates as a whole, and the critical stress τ_c increases.

Figure 6 demonstrates that for $d/L<0.2$, individual inclusions can promote GB migration. In the examined two-dimensional model, this range of *d/L* corresponds to the range $r < 0.04$, where *r* is the ratio of the inclusion volume to the volume of the grain. Although the estimate $r < 0.04$ for the normalized volume of inclusions which can promote GB migration is valid in the two-dimensional model, it is logical to assume that this estimate can also be extended to the case of three-dimensional grains and inclusions. At the same time, even small inclusions can hinder migration of low-angle GBs, if the concentration of inclusions is high, so that each grain contains a large number of nanoinclusions. In this situation, the total length of moving GB segments can be significantly reduced by nanoinclusions, which should increase the critical stress for unlimited GB migration and thus hamper grain growth. The exact relation between the critical parameters of the inclusions (their critical volume fraction critical size) below which inclusions can promote migration of low-angle GBs cannot, however, be found within our model.

Finally, let us consider the stress-driven GB migration as a plastic deformation mode in metal matrix nanocomposites containing incoherent reinforcing nanoinclusions. To do so, we roughly estimate the average plastic strain ε produced by migrating GBs. In the first approximation, this plastic strain can be presented as $\varepsilon = (\alpha\,\bar{\omega}\,\bar{s}/d)f$, where α is the geometric factor (of the order of unity) arising as a result of the averaging of plastic strain over various orientations of migrating low-angle GBs, $\bar{\omega}$ is the average misorientation angle of the migrating low-angle GBs, $\bar{s}$ is their average migration distance, *d* is average grain size, and *f* is the fraction of low-angle GBs. In order to estimate the average plastic strain, let us put $\alpha = 0.5$, $\omega = 10°$, and $f = 0.3$. Then, in the limited case of a very high applied stress at which all GBs move unlimitedly (in reality, across one grain), we obtain $\bar{s}/d = 1$, which yields $\varepsilon = 0.026$. In the case where the average migrating distance is much smaller than the grain size ($\bar{s}/d = 0.1$), we obtain $\varepsilon = 0.0026$. The above estimates demonstrate that in the discussed cases, the macroscopic plastic strain produced by pre-existent migrating low-angle GBs is small. Therefore, stress-driven migration of low-angle GBs should occur in parallel with other deformation mechanisms. At the same time, note that the above estimates describe the contributions of pre-existent low-angle GBs, while plastic deformation can be accompanied by the formation of new low-angle GBs as a result of accumulation of lattice dislocations in dislocation walls [10] and/or due to splitting of the existing GBs [59]. Also, if migration of high-angle GBs can occur in parallel with the migration of low-angle ones,

such migration can significantly increase the contribution of GB migration to the total plastic strain. Thus, migration of GBs contributes to the total plastic deformation and, therefore, can be considered as a particular deformation mode.

Concluding remarks

To summarize, in metal matrix nanocomposites with reinforcing (metallic or ceramic) incoherent nanoinclusions, stress-driven migration of GBs represents a special deformation mode significantly influenced by these nanoinclusions. In this paper, we theoretically examined a rather widespread situation where low-angle tilt boundaries migrate under a shear stress, and nanoinclusions cannot be penetrated by migrating GBs. In this situation, according to the results of our theoretical analysis, the stress-driven GB migration in the nanocomposite can occur in the limited and unlimited modes. In the limited migration mode, migrating GBs eventually approach their equilibrium positions corresponding to a given value of the applied stress (Figs. 4a, b, 5a, 7). In the unlimited migration mode, some segments of a migrating GB stop at the nanoinclusion boundary, while others move unrestrictedly far away from the nanoinclusion (Figs. 4c, 5b). (In real materials, GBs exhibiting the unlimited migration mode are stopped by their neighboring GBs.) The transition from limited to unlimited GB migration occurs at some critical value of the applied shear stress. This critical stress serves as the key characteristic for the effects exhibited by nanoinclusions on the stress-driven GB migration in nanocomposites. Our analysis demonstrated that in the examined case of a nanocomposite containing nanoinclusions, the critical stress significantly depends on such geometric parameters as the ratio d/L. In particular, surprisingly, it has been found that for small values of d/L, the critical stress decreases with the rise in nanoparticle size d (Fig. 6). This means that small nanoparticles in a moderate concentration can promote migration of low-angle GBs. At the same time, for comparatively large values of d/L, the critical stress grows with an increase in the ratio d/L, as one could expect (Fig. 6). This implies that large enough nanoinclusions hinder GB migration.

In general, it would be interesting to compare the presented theoretical results with experimental data. However, since experimental research in this area is in its infancy, comparison of such a kind is very limited. So, as to our knowledge, there are only experiments [44, 45] concerning the effects of ceramic incoherent nanoinclusions on the stress-driven GB migration in nanostructured metal matrix composites. These experiments showed that (i) thermally activated grain growth is effectively suppressed by Al_2O_3 ceramic nanoinclusions in these composites having nanostructured metal (Al or Al-based alloy) matrixes under thermal treatment for several hours at elevated temperature (600 °C); (ii) grain growth effectively occurs through both stress-driven GB migration and grain rotation processes in nanostructured metal–Al_2O_3 nanocomposites under mechanical treatment. These experimental data are consistent with our theoretical prediction that the stress-driven GB migration in metal matrix nanocomposites reinforced by (ceramic or metallic) incoherent nanoinclusions occurs at some critical stress. That is, in agreement with the experimental data [44, 45], in the absence of a mechanical load, GB migration is suppressed. Also, in agreement with the same experiments, we theoretically predict that the stress-driven GB migration occurs when the external critical stress is applied. However, other theoretical predictions presented here still wait for comparison with future experiments in this new area of nanomaterials science. Besides, the theoretical model formulated in this paper can be modified for the scientifically interesting case of high-angle GBs migrating in metal matrix nanocomposites reinforced by nanoinclusions of the second phase. This modification will be the subject of our future examinations.

Acknowledgements This work was supported by the Russian Science Foundation (Research Project 14-29-00199).

References

1. Koch CC (2007) Structural nanocrystalline materials: an overview. J Mater Sci 42:1403–1414
2. Kawasaki M, Langdon TG (2007) Principles of superplasticity in ultrafine-grained materials. J Mater Sci 42:1782–1796
3. Ovid'ko IA (2007) Review on the fracture processes in nanocrystalline materials. J Mater Sci 42:1694–1708
4. Koch CC, Ovid'ko IA, Seal S, Veprek S (2007) Structural Nanocrystalline Materials: Fundamentals and Applications. Cambridge University Press, Cambridge
5. Ovid'ko IA, Sheinerman AG (2009) Enhanced ductility of nanomaterials through optimization of grain boundary sliding and diffusion processes. Acta Mater 57:2217–2228
6. Pande CS, Cooper KP (2009) Nanomechanics of Hall-Petch relationship in nanocrystalline materials. Progr Mater Sci 54:689–706
7. Abdolrahim N, Mastorakos IN, Zbib HM (2010) Deformation mechanisms and pseudoelastic behaviors in trilayer composite metal nanowires. Phys Rev B 81:054117
8. Abdolrahim N, Mastorakos IN, Zbib HM (2012) Precipitate strengthening in nanostructured metallic material composites. Philos Mag Lett 92:597–607
9. Zhu YT, Liao XZ, Wu X-L (2012) Deformation twinning in nanocrystalline materials. Progr Mater Sci 57:1–62
10. Estrin Y, Vinogradov A (2013) Extreme grain refinement by severe plastic deformation: a wealth of challenging science. Acta Mater 61:782–817
11. Abdolrahim N, Zbib HM, Bahr DF (2014) Multiscale modeling and simulation of deformation in nanoscale metallic multilayer systems. Int J Plasticity 52:33–50

12. Jin M, Minor AM, Stach EA, Morris JW Jr (2004) Direct observation of deformation-induced grain growth during the nanoindentation of ultrafine-grained Al at room temperature. Acta Mater 52:5381–5387
13. Soer WA, De Hosson JTM, Minor AM, Morris JW Jr, Stach EA (2004) Effects of solute Mg on grain boundary and dislocation dynamics during nanoindentation of Al–Mg thin films. Acta Mater 52:5783–5790
14. Gutkin MY, Ovid'ko IA (2005) Grain boundary migration as rotational deformation mode in nanocrystalline materials. Appl Phys Lett 87:251916
15. Gianola DS, Van Petegem S, Legros M, Brandstetter S, Van Swygenhoven H, Hemker KJ (2006) Stress-assisted discontinuous grain growth and its effect on the deformation behavior of nanocrystalline aluminum thin films. Acta Mater 54:2253–2263
16. Cahn JW, Mishin Y, Suzuki A (2006) Coupling grain boundary motion to shear deformation. Acta Mater 54:4953–4975
17. Sansoz F, Dupont V (2006) Grain growth behavior at absolute zero during nanocrystalline metal indentation. Appl Phys Lett 89:111901
18. Gai PL, Zhang K, Weertman J (2007) Electron microscopy study of nanocrystalline copper deformed by a microhardness indenter. Scripta Mater 56:25–28
19. Pan D, Kuwano S, Fujita T, Chen MW (2007) Ultra-large room-temperature compressive plasticity of a nanocrystalline metal. Nano Lett 7:2108–2111
20. Ivanov VA, Mishin Y (2008) Dynamics of grain boundary motion coupled to shear deformation: an analytical model and its verification by molecular dynamics. Phys Rev B 78:064106
21. Ovid'ko IA, Sheinerman AG, Aifantis EC (2008) Stress-driven migration of grain boundaries and fracture processes in nanocrystalline ceramics and metals. Acta Mater 56:2718–2727
22. Rupert TJ, Gianola DS, Gan Y, Hemker KJ (2009) Experimental observations of stress-driven grain boundary migration. Science 326:1686–1690
23. Ovid'ko IA, Sheinerman AG, Aifantis EC (2011) Effect of cooperative grain boundary sliding and migration on crack growth in nanocrystalline solids. Acta Mater 59:5023–5031
24. Bobylev SV, Morozov NF, Ovid'ko IA (2010) Cooperative grain boundary sliding and migration process in nanocrystalline solids. Phys Rev Lett 105:055504
25. Cheng S, Zhao Y, Wang Y, Li Y, Wang X-L, Liaw PK, Lavernia EJ (2010) Structure modulation driven by cyclic deformation in nanocrystalline NiFe. Phys Rev Lett 104:255501
26. Molodov DA, Gorkaya T, Gottstein G (2011) Dynamics of grain boundaries under applied mechanical stress. J Mater Sci 46:4318–4326
27. Mompiou F, Legros M, Caillard D (2011) Direct observation and quantification of grain boundary shear-migration coupling in polycrystalline Al. J Mater Sci 46:4308–4313
28. Bobylev SV, Ovid'ko IA (2012) Grain boundary rotations in solids. Phys Rev Lett 109:175501
29. Trautt ZT, Adland A, Karma A, Mishin Y (2012) Coupled motion of asymmetrical tilt grain boundaries: molecular dynamics and phase field crystal simulations. Acta Mater 60:6528–6546
30. Karma A, Trautt ZT, Mishin Y (2012) Relationship between equilibrium fluctuations and shear-coupled motion of grain boundaries. Phys Rev Lett 109:095501
31. Yu M, Fang Q, Feng H, Liu Y (2014) Effect of cooperative grain boundary sliding and migration on dislocation emitting from a semi-elliptical blunt crack tip in nanocrystalline solids. Acta Mech 225:2005–2019
32. Zhao Y, Fang Q, Liu Y (2014) Effect of cooperative nanograin boundary sliding and migration on dislocation emission from a blunt nanocrack tip in nanocrystalline materials. Philos Mag 94:700–730
33. Chan T, Zhou Y, Brooks I, Palumbo G, Erb U (2014) Localized strain and heat generation during plastic deformation in nanocrystalline Ni and Ni–Fe. J Mater Sci 49:3847–3859
34. Gregory F, Murakami K, Bacroix B (2014) The influence of microstructural features of individual grains on texture formation by strain-induced boundary migration in non-oriented electrical steels. J Mater Sci 49:1764–1775
35. Rios PR (1987) Overview no. 62: a theory for grain boundary pinning by particles. Acta Metall 35:2805–2814
36. Manohar PA, Ferry M, Chandra T (1998) Review: five Decades of the Zener Equation. ISIJ International 38:913–924
37. Kim G-H, Hong S-M, Lee M-K, Kim S-H, Ioka I, Kim B-S, Kim I-S (2010) Effect of oxide dispersion on dendritic grain growth characteristics of cast aluminum alloy. Mater Trans A 51:1951–1957
38. Guo JF, Lio J, Sun CN, Maleksaeedi S, Bi G, Tan MJ, Wei J (2014) Effects of nano-Al_2O_3 particle addition on grain structure evolution and mechanical behaviour of friction-stir-processed Al. Mater Sci Eng, A 602:143–149
39. Torizuka S, Muramatsu E, Narayana Murty SVS, Nagai K (2006) Microstructure evolution and strength-reduction in area balance of ultrafine-grained steels processed by warm caliber rolling. Scr Mater 55:751–754
40. Askari H, Zbib H, Sun X (2013) Multiscale modeling of inclusions and precipitation hardening in metal matrix composites: application to advanced high-strength steels. J Nanomech Micromech 3:24–33
41. Davidson DL (1993) Fatigue and fracture toughness of aluminium alloys reinforced with SiC and alumina particles. Composites 24:248–255
42. Feng H, Zhou Y, Dechang J, Qingchang M (2004) Microstructure and mechanical properties of in situ TiB reinforced titanium matrix composites based on Ti–FeMo–B prepared by spark plasma sintering. Comp Sci Technol 64:2495–2500
43. Li J, Fang Q, Liu Y (2013) Crack interaction with a second phase nanoscale circular inclusion in an elastic matrix. Int J Engn Sci 72:89–97
44. Lin Y, Wen H, Li Y, Wen B, Lavernia EJ (2014) Stress-induced grain growth in an ultra-fine grained Al alloy. Metall Mater Trans B 45:795–810
45. Lin Y, Xu B, Feng Y, Lavernia EJ (2014) Stress-induced grain growth during high-temperature deformation of nanostructured Al containing nanoscale oxide particles. J Alloys and Compounds 596:79–85
46. Dám K, Lejček P (2013) In situ TEM investigation of microstructural behavior of superplastic Al–Mg–Sc alloy. Mater Charact 76:69–75
47. Lin Y, Wen H, Li Y, Wen B, Wei L, Lavernia EJ (2015) An analytical model for stress-induced grain growth in the presence of both second-phase particles and solute segregation at grain boundaries. Acta Mater 82:304–315
48. Zálezák T, Dlouhý A (2012) 3D discrete dislocation dynamics applied to interactions between dislocation walls and particles. Acta Phys Pol, A 122:450–452
49. Gianola DS, Farkas D, Gamarra M, He M (2012) The role of confinement on stress-driven grain boundary motion in nanocrystalline aluminum thin films. J Appl Phys 112:124313
50. Tengen TB (2012) The response of the statistics of the cumulative features on grains in nanomaterials to different grain growth phenomena. Int J Mech Mater Des 8:101–112
51. Aramfard M, Deng C (2014) Influences of triple junctions on stress-assisted grain boundary motion in nanocrystalline materials. Model Simul Mater Sci Eng 22:055012
52. Sutton AP, Balluffi RW (1995) Interfaces in Crystalline Materials. Clarendon, Oxford, pp 70–96

53. Bollmann W (1984) Triple lines in polycrystalline aggregates as disclinations. Philos Mag A 49:73–79
54. Bollmann W (1988) Triple-line disclinations: representations, continuity and reactions. Philos Mag A 57:637–649
55. Ovid'ko IA, Sheinerman AG (2014) Stress-driven migration of low-angle tilt boundaries in nanocrystalline and ultrafine-grained metals containing coherent nanoinclusions. Rev Adv Mater Sci 39:99–107
56. Bobylev SV, Gutkin MY, Ovid'ko IA (2004) Decay of low-angle tilt boundaries in deformed nanocrystalline materials. J Phys D 37:269–272
57. Bobylev SV, Gutkin MY, Ovid'ko IA (2004) Transformations of grain boundaries in deformed nanocrystalline materials. Acta Mater 52:3793–3805
58. Rzhavtsev EA, Gutkin MY (2015) The dynamics of dislocation wall generation in metals and alloys under shock loading. Scripta Mater 100:102–105
59. Bobylev SV, Ovid'ko IA (2015) Stress-driven migration of deformation-distorted grain boundaries in nanomaterials. Acta Mater 88:260–270
60. Bulatov V, Cai W (2006) Computer Simulations of Dislocations. Oxford University Press, Oxford
61. Groh S, Zbib M (2009) Advances in discrete dislocation dynamics and multiscale modeling. J Ing Mater Tech 131:041209
62. Arsenlis T, Bulatov VV, Cai W, Hommes G, Rhee M, Tang M (2011) Documentation of ParaDiS V2. 5. 1
63. Zbib HM (2012) Introduction to discrete dislocation dynamics. In: Sansour C, Skatulla S (eds) CISM Cources and Lectures, vol 537. Springer, New York, pp 289–317 Generalized Continua and Dislocation Theory
64. Kocks UF, Argon AS, Ashby MF (1975) Thermodynamics and kinetics of slip. Prog Mater Sci 19:1–288
65. Hirth JP, Lothe J (1982) Theory of Dislocations. Wiley, New York